

Ultra-Uniformity in Nanocrystalline Materials: Implications from Generalized Growth Theory and Validations

Yanhao Dong¹ (dongyh@mit.edu), Hongbing Yang², Jiangong Li², Ju Li^{1,3}, I-Wei Chen⁴

¹*Department of Nuclear Science and Engineering, Massachusetts Institute of Technology, Cambridge, MA 02139, USA*

²*Institute of Materials Science and Engineering and MOE Key Laboratory for Special Functional Materials and Structure Design, Lanzhou University, Lanzhou 730000, China*

³*Department of Materials Science and Engineering, Massachusetts Institute of Technology, Cambridge, MA 02139, USA*

⁴*Department of Materials Science and Engineering, University of Pennsylvania, Philadelphia, PA 19104, USA*

Keywords: Nanocrystalline materials, microstructure, grain growth, alumina

Nanocrystalline materials with <100 nm grain size in the form of metals, ceramics and other functional materials often show superior properties and are thus of great interest. Much has been discussed about ultrafine grain sizes, but little is known about ultra-uniformity, defined as grain size distribution narrower than the theoretical prediction of Hillert for dense polycrystals. Here we provide a generalized growth theory unifying the mean-field solutions from

Lifshitz, Slyozov, Wagner (LSW)^{1,2} and Hillert³. For curvature driven grain growth, we find for growth exponent $n>1$ a steady-state size distribution that is analytically solvable. Significantly, the distribution narrows with increasing n , which can be beneficially utilized to homogenize the microstructure. This proposal is experimentally validated in dense Al₂O₃ with an extremely uniform microstructure of 34 nm average grain size.

Rapid development of nanocrystalline materials in the past decades provides much room for improved and emerging properties at the bottom. While a fine average grain size is typically used to describe the benefits for nano-structuring (e.g. Hall-Petch relationship for grain boundary strengthening), the size distribution also matters especially in terms of engineering reliability. This is because failure events, being mechanical or electrical, from instantaneous breakdown to slow degradation, all happen at the weakest point, which comes from microstructural or chemical inhomogeneity and could simply be at some abnormally large grains in polycrystalline materials. Therefore, achieving a narrow grain size distribution in nanocrystalline materials is of great technologically interests. From this perspective, the theoretical limit of the normalized grain size distribution in dense polycrystals is probably the one given by Hillert, which assumes all the grain boundaries have the same energy and mobility. In fact, for any real materials, this assumption cannot be exactly true, which is the reason why numerous experimental studies found much broader size distributions than Hillert's and abnormally large grains beyond Hillert's

upper cut-off grain size, especially in materials with strong anisotropy and complicated grain boundary structure/chemistry. This consensus shall be challenged in the present work. We were inspired by the steady-state size distribution we recently obtained for the generalized growth problem with size-dependent mobility (including the ones from LSW and Hillert as two special cases), and proposed that ultra-uniform microstructure beyond Hillert’s limit can be achieved in the porous form which is known to have a large growth exponent $n \geq 3$. It follows that ultra-uniform microstructure can be realized in dense samples if grain structure in porous samples can be frozen upon further densification. We shall experimentally validate this proposal in alumina (Al_2O_3) ceramics, which is not known to be uniform at all and has probably the most complicated scattering grain boundary structure, chemistry and properties (including grain boundary mobility)—both lying at the other extreme of a “good” demonstrator for the mean-field prediction.

Theory of microstructure coarsening to minimize the total interfacial energy was first formulated by Lifshitz, Slyozov and Wagner (LSW) for precipitates in 1961. This capillary process dictates a critical particle size G_{cr} , above which the precipitates grow and below which the precipitates shrink, in what is commonly referred to as the Oswald ripening process. Grain growth in a dense polycrystal was similarly analyzed by Hillert in 1965. As the capillary driving force decreases with the feature size, the coarsening rate characteristically decreases with time. The LSW theory predicts a cubic growth law (i.e., average size G_{avg} and time t follows $G_{\text{avg}}^3 \sim t$) for bulk diffusion-controlled precipitate coarsening, which has been verified experimentally.

Hillert's prediction—parabolic law $G_{\text{avg}}^2 \sim t$ for normal grain growth controlled by boundary migration—is more difficult to verify because of crystallographic texture and substructure pinning, by sub-grain walls, pores and second phase particles, yet it has been convincingly demonstrated in high-density ceramics, with few pores and little residual stress. In Hillert's theory, the growth rate (i.e., the equation of motion) for each individual grain with size G under a capillary driving force $2\gamma/G$ with γ being the interfacial energy is written as

$$\frac{dG}{dt} = 2M_b\gamma \left(\frac{1}{G_{\text{cr}}} - \frac{1}{G} \right) \quad (1)$$

Here, M_b is the mobility of grain boundary, and G_{cr} is the critical grain size that neither grows nor shrinks at time t thus setting up a chemical potential $2\gamma/G_{\text{cr}}$ for the system that ensures mass (volume) conservation. We now generalize Eq. (1) with a

size-dependent effective mobility $M \left(\frac{G}{a} \right)^\alpha$ and express the equation of motion as

$$\frac{dG}{dt} = 2M\gamma \left(\frac{G}{a} \right)^\alpha \left(\frac{1}{G_{\text{cr}}} - \frac{1}{G} \right) \quad (2)$$

with a being the atomic spacing to preserve the dimension. Obviously, Hillert's solution corresponds to $\alpha=0$ and LSW's precipitate coarsening corresponds to $\alpha=-1$

by letting $M = \frac{D}{k_B T} \frac{\Omega}{a}$, where D is the diffusivity, Ω is the atomic volume and $k_B T$

has their usual meaning. Following the analytical method of LSW and Hillert, we recently showed that a steady-state solution exists for arbitrary $\alpha \leq 1$, where a power-form growth law $G_{\text{avg}}^n \sim t$ with growth exponent $n=2-\alpha$ and a normalized size distribution $P'(u)$ in the following closed form are asymptotically approached.⁴

$$P'(u) = \frac{3u^{1-\alpha}}{u^{2-\alpha} - \frac{(2-\alpha)^{2-\alpha}}{(1-\alpha)^{1-\alpha}}(u-1)} \exp \left[-\frac{3}{2-\alpha} \int_0^u \frac{-(2-\alpha)u^{1-\alpha}}{\frac{(2-\alpha)^{2-\alpha}}{(1-\alpha)^{1-\alpha}}(u-1) - u^{2-\alpha}} du \right] \quad (3)$$

Here, for convenience, the normalized grain size G/G_{avg} is multiplied by

$u_{\text{avg}} = \int_0^{u_0} u P'(u) du$ to form a new variable $u = \frac{G}{G_{\text{avg}}} u_{\text{avg}}$, and the corresponding

normalized size distribution $P(G/G_{\text{avg}})$ can be obtained from $P'(u)$ by change of variable.

Several examples of calculated $P(G/G_{\text{avg}})$ with different α are presented in **Fig. 1** (corresponding $P'(u)$ shown in **Fig. S3**), including the ones from LSW (in red, $\alpha=-1$) and Hillert (in blue, $\alpha=0$). A key feature of interest is that $P(G/G_{\text{avg}})$ becomes more extended as α increases or equivalently as n decreases. To the first-order approximation, this dispersion can be quantified by the standard deviation σ of G/G_{avg} . As shown by the inset of **Fig. 1**, σ monotonically increases with increasing α (and thus with decreasing n), reaching a maximum of 1.0 at $\alpha=1$ ($n=1$), beyond which there is no more a steady state and σ is likely to diverge when size bifurcation takes over. Consistently, the normalized upper cut-off size $G_{\text{max}}/G_{\text{avg}}$ also increase with α and go to infinity at $\alpha=1$ (**Fig. S2**), which is another indicator of the dispersity. This theoretical prediction provides us a guidance to achieve ultra-uniformity: promote grain growth with large growth exponent n and suppress growth with small n (e.g., in the dense form with $n=2$). In practice, the former is known to hold in porous materials where $n \geq 3$ has been frequently reported for pore-containing ceramics, because a larger grain boundary would be statistically in contact with more pores and sense a

stronger pinning force. Therefore, we propose grain growth in porous materials may have a narrower size distribution than the one after extensive grain growth in dense samples, which can be beneficially utilized to homogenize the microstructure. If this distribution can be preserved upon further densification, ultra-uniformity in dense materials can be realized.

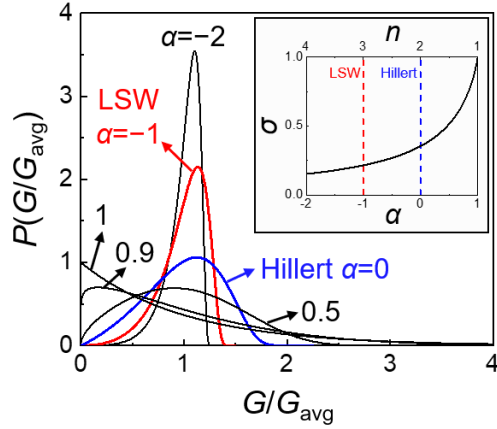


Figure 1 Steady-state solution of generalized growth problem. Calculated normalized grain size distribution function $P(G/G_{\text{avg}})$ as a function of α . Inset: Calculated standard deviations σ for G/G_{avg} as a function of α and n .

We now provide the first experimental comparison of grain size distributions between porous and dense samples. The first set of data were obtained in high-purity Al_2O_3 ceramics, which are pressurelessly sintered to different densities at various temperatures without holding. As shown by filled circles in **Fig. 2a** are the average grain size G_{avg} and its standard deviation (as error bar) measured from transmission electron microscopy (TEM) images of fractured fragments. While G_{avg} obviously grows with increasing relative density ρ , there is also simultaneous increase of its

standard deviation. Similar trend holds in **Fig. 2b**, where open circles represent the data collected from the same samples but measured from scanning electron microscopy (SEM) images of fractured and thermally etched surfaces. Notwithstanding the evolving sizes, we compared their σ (i.e., standard deviation of normalized grain size G/G_{avg}) in **Fig. 2c** (filled circles from TEM data and open circles from SEM data) and found σ increases concavely with $\rho > 65\%$ as densification proceeds, indicating progressively broadening of the size distribution. Upon further annealing after full density is reached, we found even larger σ (open diamonds in green in **Fig. 2c**, measured from SEM) when grain growth takes place in dense samples. For illustration, the microstructure (**Fig. 3a**) and normalized grain size distribution (**Fig. 3b**) of 84% density sample (sintered at 1150 °C without holding) are compared with the ones (**Fig. 3e-f**) of fully dense sample sintered at 1300 °C for 10 h, the former of which show better uniformity than the latter. As further demonstrations, we also compared pressurelessly sintered porous ($\rho=69\%$) and dense 8 mol% yttria stabilized zirconia (8YSZ; σ plotted in **Fig. 2c** by orange squares, measured from SEM of polished and thermally etched surfaces; microstructures and normalized grain size distribution of porous and dense samples shown by **Fig. 3g-h** and **Fig. 3i-j**, respectively), which is much more uniform for the former than the latter. Therefore, the question is settled: porous samples do have smaller σ hence narrower size distributions than dense ones. Such a small σ (even below Hillert's limit of 0.354) naturally benefits from the narrowly dispersed initial powders, but it cannot explain all because (i) multifold (>10) coarsening takes place during densification and (ii)

Al_2O_3 's data in **Fig. 2c** show larger σ for $\rho < 65\%$ than that for $65\% < \rho < 85\%$. So it is indeed the grain growth in the porous form that plays a major role to narrow down the size distribution, which agrees with our theoretical prediction.

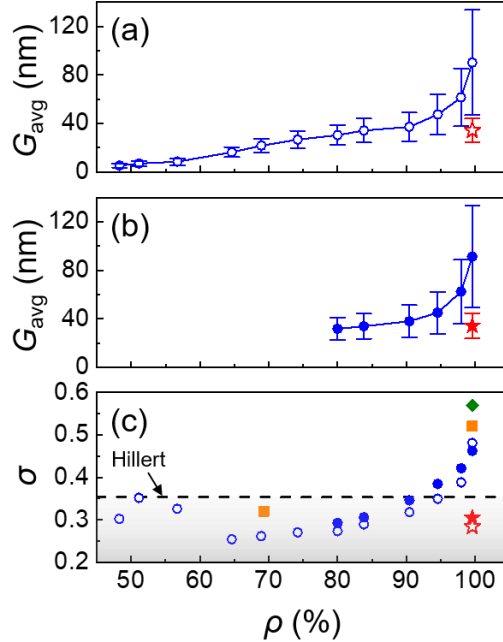


Figure 2 Microstructural dispersity in porous and dense polycrystals. Average grain size G_{avg} -relative density ρ trajectory of Al_2O_3 ceramics measured from (a) TEM in open symbols and (b) SEM in closed symbols. Normal sintering data in blue and two-step sintering data in red. Their standard deviations σ for G/G_{avg} are plotted in (c). Also included are σ of high-temperature annealed Al_2O_3 (diamonds in green) and 8YSZ (squares in orange).

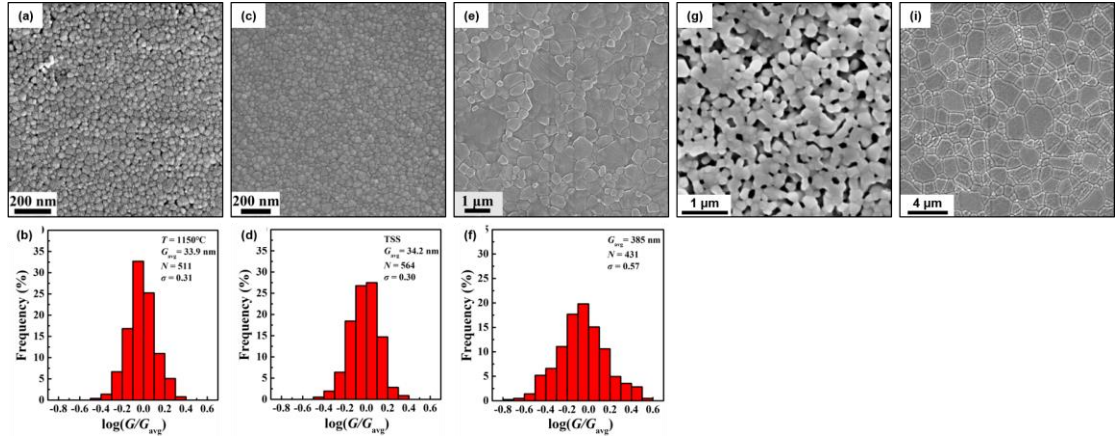


Figure 3 Comparison of microstructural uniformity. Microstructures and normalized grain size distributions of (a-b) Al_2O_3 sintered at 1150 °C without holding, 84% relative density; (c-d) Al_2O_3 two-step sintered at 1150 °C without holding and then at 1025 °C for 40 h, fully dense; (e-f) Al_2O_3 sintered at 1300 °C for 10 h, fully dense; (g-h) 8YSZ sintered at 1280 °C without holding, 69% relatively density; and (i-j) 8YSZ sintered at 1300 °C for 12 h, fully dense. Also listed are G_{avg} , σ , and number N of measured grains.

The remaining question is whether the narrow size distribution in the porous samples can be preserved to dense ones, because it is ultra-uniform dense samples that are most useful. We show this possibility by pressureless two-step sintering of Al_2O_3 first at 1150 °C without holding (reaching $\rho=84\%$), then cool down to 1025 °C and hold for 40 h. It provides fully dense Al_2O_3 ($\rho=99.6\%$) with $G_{\text{avg}}=34$ nm and $\sigma=0.30$ (microstructure in **Fig. 3c** and normalized grain size distribution in **Fig. 3d**), both of which are similar to their corresponding values in 84% density sample ($G_{\text{avg}}=34$ nm and $\sigma=0.31$; **Fig. 3a-b**). Therefore, dense ultra-uniform nanocrystalline Al_2O_3 demonstrated. Lastly, we address the generalizability of our proposed strategy by the

constructed Ashby plot of G_{avg} and σ in **Fig. 4**. Compared to other processing techniques, two-step sintering—which suppress grain growth in later stage sintering $\rho > 70\text{-}80\%$ —provides not only smaller average grain size, but also smaller σ hence more uniform microstructure and improved properties. As concluding remarks, we consider the new theoretical insights provided in this work and the demonstrated ultra-uniformity are helpful to the future development of dense nanocrystalline materials and more detailed studies of their structure-properties relationship—though monodispersed grain size distribution in dense samples remains challenging.

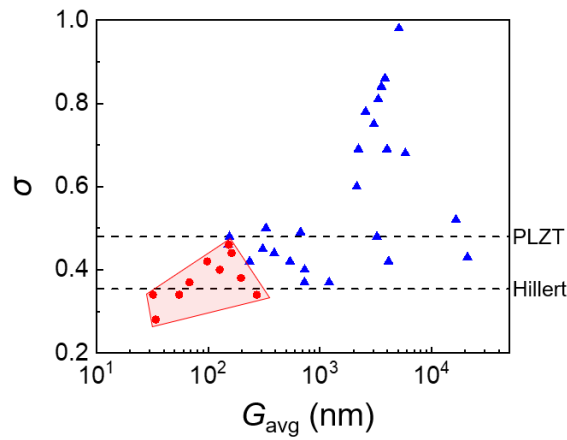


Figure 4 Ashby plot for average grain size G_{avg} vs. standard deviation σ of normalized grain size. Comparison of G_{avg} and σ of various sintered ceramics, including our data and literature ones. (Two-step sintering data by red circles and others by blue triangles; details available in **Supplementary Table S1**.) Classical reference of PLZT and Hillert's theoretical prediction are shown by dash lines.

References

[1] I.M. Lifshitz, V.V. Slyozov, The Kinetics of Precipitation from Supersaturated

Solid Solutions, J. Phys. Chem. Solids 19 (1961) 35-50.

[2] C.Z. Wagner, Theorie der Alterung von Niederschlägen durch Umlösen

(Ostwald-reifung), Berichte der Bunsengesellschaft für physikalische Chemie 65

(1961) 581-591.

[3] M. Hillert, On the Theory of Normal and Abnormal Grain Growth, Acta Mater. 13

(1965) 227-238.

[4] Y. Dong, I.W. Chen, Grain growth with size-dependent or statistically distributed

mobility, arXiv preprint arXiv:1708.04092 (2017).

Supplementary information

Ultra-uniformity in Nanocrystalline Materials: Implications from Generalized LSW Growth Theory and Validations

Yanhao Dong¹, Hongbing Yang², Jiangong Li², Ju Li^{1,3}, I-Wei Chen⁴

¹*Department of Nuclear Science and Engineering, Massachusetts Institute of Technology, Cambridge, MA 02139, USA*

²*Institute of Materials Science and Engineering and MOE Key Laboratory for Special Functional Materials and Structure Design, Lanzhou University, Lanzhou 730000, China*

³*Department of Materials Science and Engineering, Massachusetts Institute of Technology, Cambridge, MA 02139, USA*

⁴*Department of Materials Science and Engineering, University of Pennsylvania, Philadelphia, PA 19104, USA*

Table of content

Supplementary Figures S1-S4

Page 2

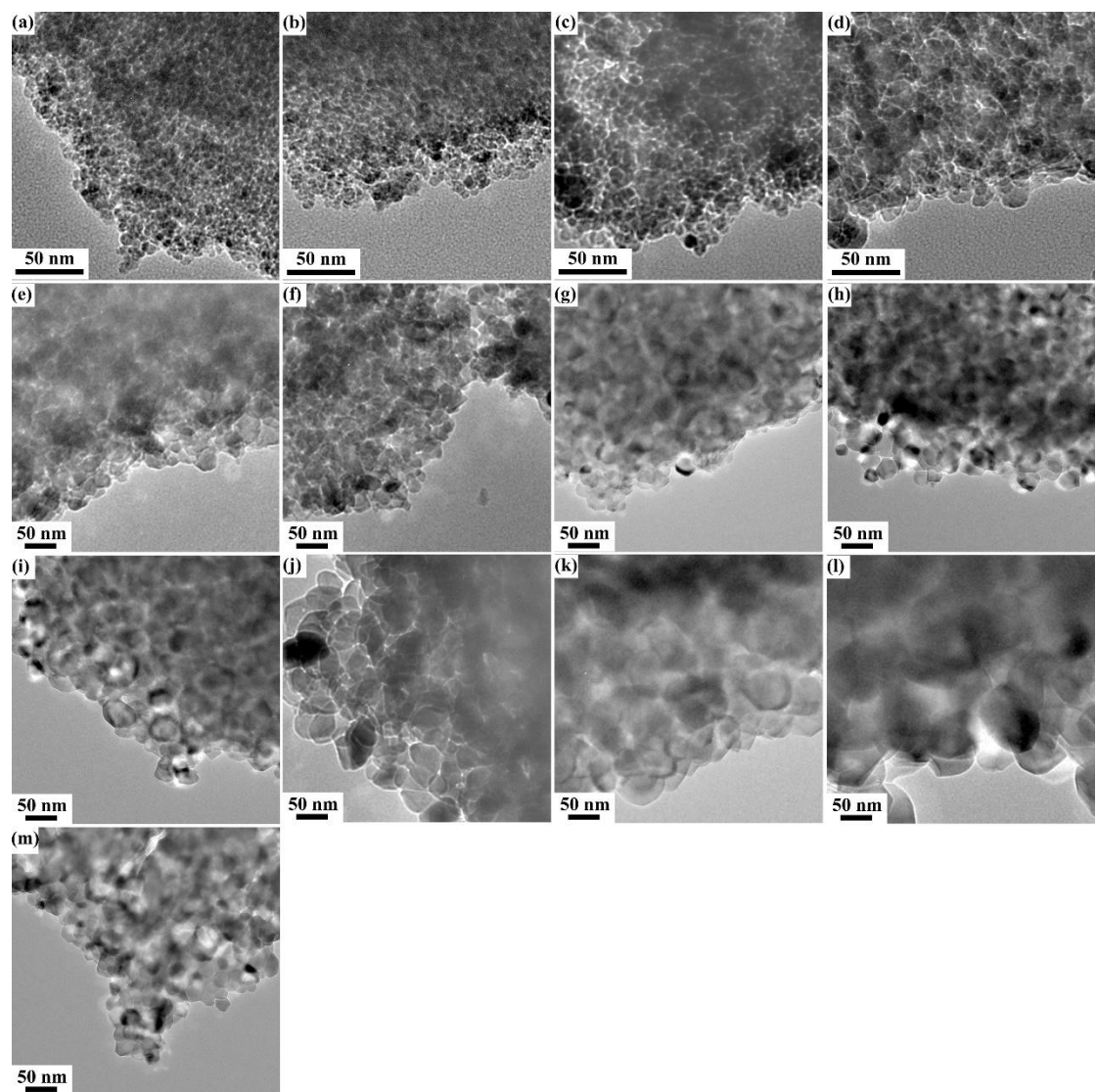


Figure S1 TEM images of Al₂O₃ sintered at different temperatures without holding.

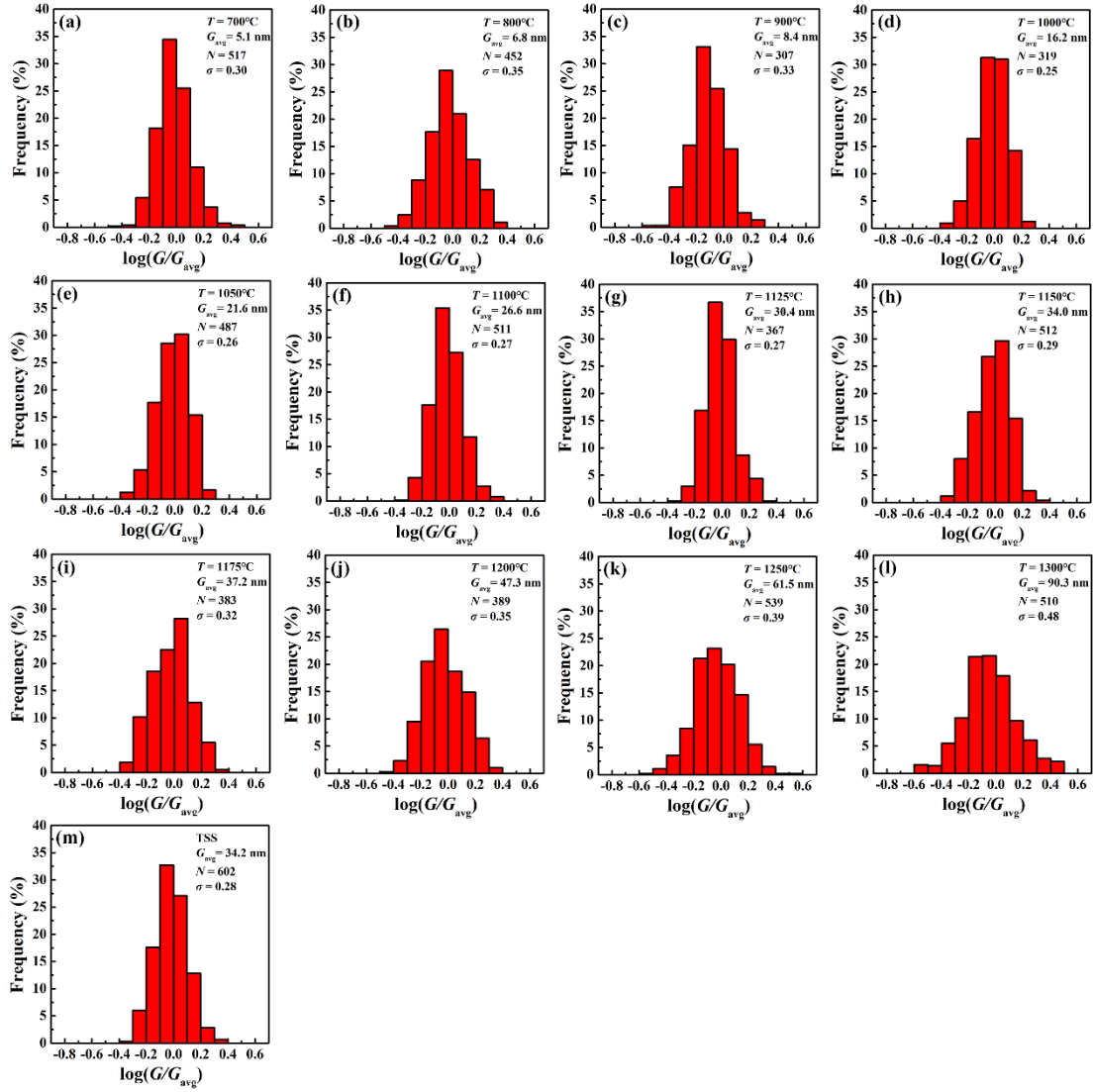


Figure S2 Normalized grain size distribution measured from TEM images in **Fig. S1**.

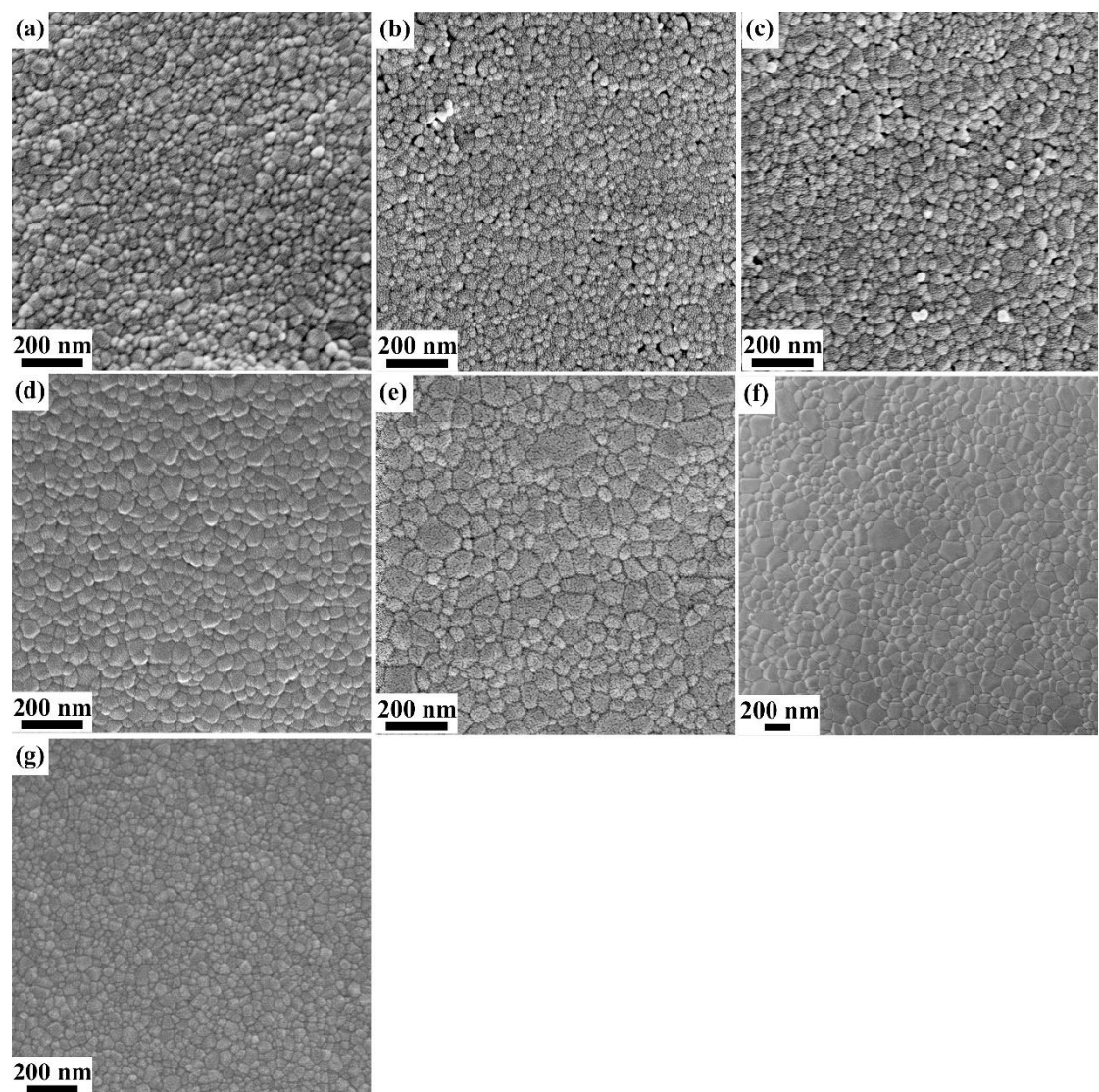


Figure S3 SEM images of Al₂O₃ sintered at different temperatures without holding.

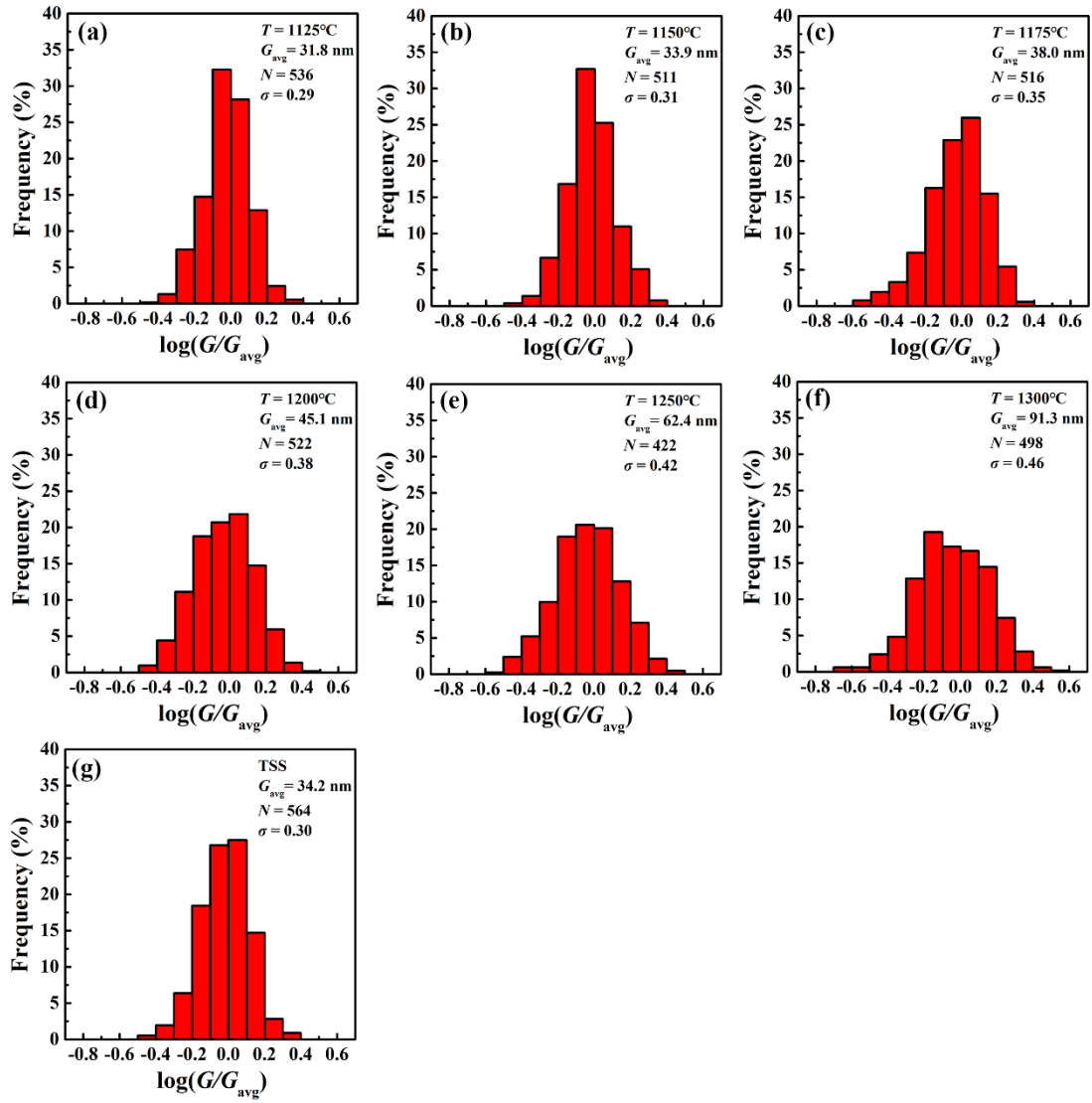


Figure S4 Normalized grain size distribution measured from SEM images in **Fig. S3**.